1981

Probable Causes of Cracking in a Series of Reinforced Concrete Box Girder Bridges

Steven Milton Bjordahl

PROBABLE CAUSES OF CRACKING IN A SERIES OF REINFORCED CONCRETE BOX GIRDER BRIDGES

BY

STEVEN MILTON BJORDAHL

A thesis submitted
in partial fulfillment of the requirements for the
degree of Master of Science, Major in
Engineering, South Dakota
State University
1974

PROBABLE CAUSES OF CRACKING IN A SERIES OF

REINFORCED CONCRETE BOX GIRDER BRIDGES

This thesis is approved as a creditable and independent investigation by a candidate for the degree, Master of Science, and is acceptable for meeting the thesis requirements for this degree. Acceptance of this thesis does not imply that the conclusions reached by the candidate are necessarily the conclusions of the major department.

Dr. Arden Sigl, Ph.D. Date
Thesis Advisor

Dr. Dwayne Rollag, Ph.D. Date
Head, Civil Engineering Dept.

ACKNOWLEDGEMENTS

The writer wishes to express his sincere gratitude for the support provided by the Civil Engineering Department and its staff, especially Dr. Sigl for his valuable assistance, the cooperation and support of the South Dakota Department of Transportation, and the understanding and encouragement of Colette, his wife.

TABLE OF CONTENTS

INTRODUCTION

Problem Statement

This thesis is the result of a study undertaken at the request of the South Dakota Department of Transportation (SDDOT) to determine the probable cause of a specific type of cracking that was observed in a series of reinforced concrete box girder bridges. The cracking consists of horizontal cracks through the end diaphragms of the girder and horizontal cracking over the interior bents. Typical crack patterns obtained from information supplied by the SDDOT are shown in Figure 1.

Historical Background

Table 1 contains a list of the bridges included in the study. As can be seen from Table 1, these bridges were completed during the period 1958 through 1961. All but one of the structures is located along Interstate 29 (I-29) between Sioux Falls and Sioux City in South Dakota. The exception, bridge number 52 436 289, is located along I-90 near Rapid City, South Dakota and was not included in the study. The bridge numbers are the bridge inventory numbers used by the SDDOT. The first two digits of the bridge numbers, 42, 50, 52 and 64, represent Lincoln, Minnehaha, Pennington and Union counties in South Dakota, respectively. The second and third groups of digits in the bridge numbers give the distances east and south, respectively,

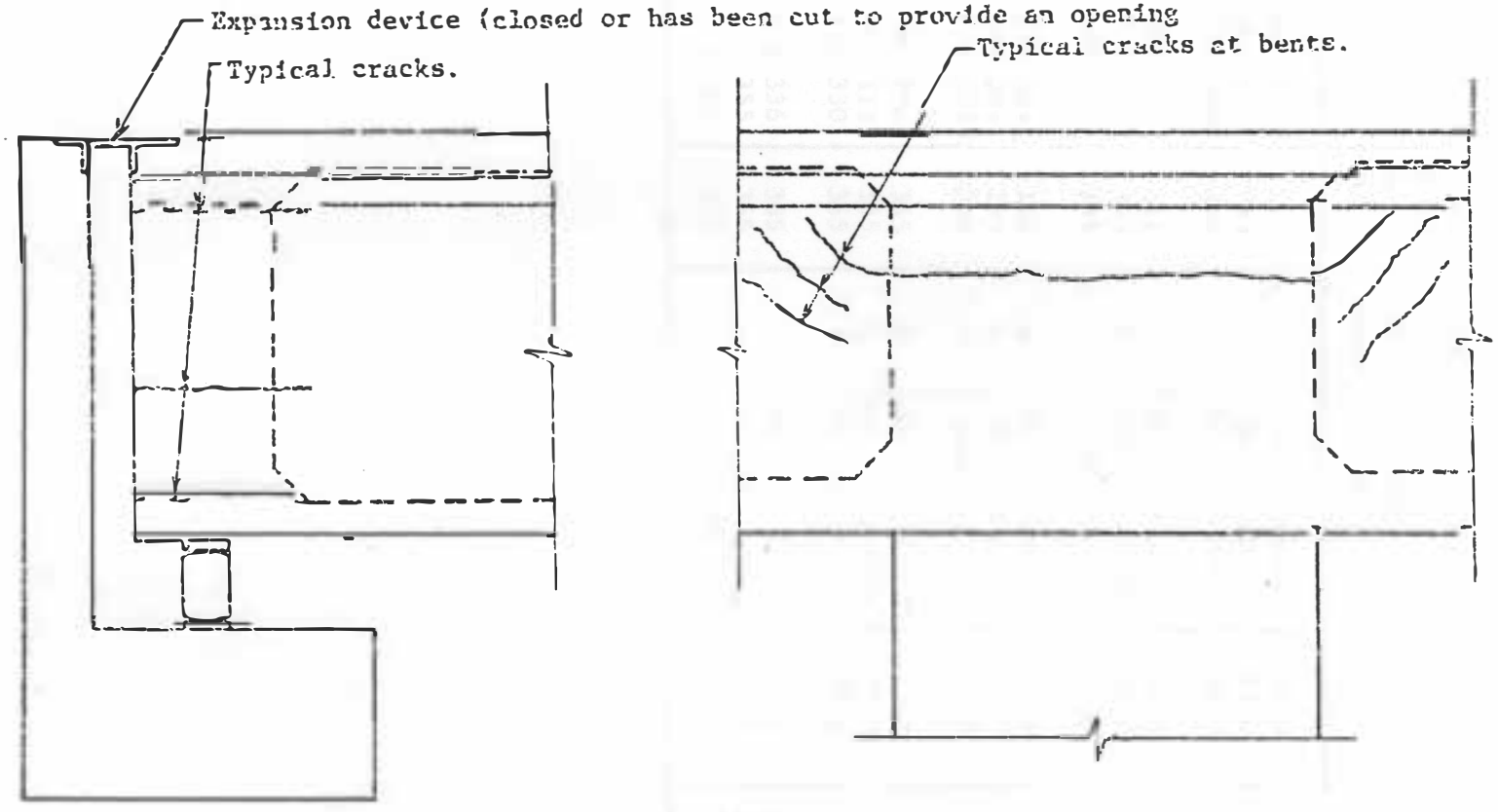

Figure 1 Typical Crack Patterns at Abutments and Bents from Information Supplied by SDDOT.

Table 1 Inventory List of the Structures Included in the Study.

Bridge No.	Bridge Length (ft.)	Number of Spans	Span Lengths (ft.)	Bridge Roadway Width (ft.)	Deck Width (ft.)	Year Built
42 065 140	293	4	64-80-80-64	30.0	34.3	1958
42 065 141	293	4	64-80-80-64	30.0	34.3	1958
42 066 006	365	4	80-100-100-80	30.0	34.3	1958
42 067 006	365	4	80-100-100-80	30.0	34.3	1958
50 178 190	365	4	80-100-100-80	30.0	34.3	1959
50 180 189	265	3	80-100-80	30.0	34.3	1959
52 436 289	365	4	80-100-100-80	30.0	34.3	1959
64 008 295	293	4	64-80-80-64	30.0	34.3	1960
64 070 287	293	4	64-80-80-64	30.0	34.3	1960
64 080 296	365	4	80-100-100-80	24.0	28.0	1961
64 100 315	365	4	80-100-100-80	24.0	28.0	1961
64 115 330	365	4	80-100-100-80	30.0	34.3	1961
64 120 336	365	4	80-100-100-80	24.0	28.0	1961
64 140 355	365	4	80-100-100-80	30.0	34.3	1961
64 149 367	293	4	64-80-80-64	30.0	34.3	1961

from the northwest corner of the county in which the bridge is located in units of tenths of miles. All but two of the structures included in the study carry traffic over I-29. The two exceptions are twin structures that carry I-29 traffic over I-229 near Sioux Falls.

Inspections of these structures for which documentation has been kept on file date back to 1969. The inspections have continued at intervals of about two years. The cracks of concern were observed in the initial inspectons.

A common element to nearly all the bridges in addition to the cracking, is that the end abutments appear to have shifted in a translatory mode toward the girders. This movement tends to close the expansion joints at the ends of the bridge which subjects the girder to a loading for which it was not designed.

Structural Details

As can be seen by inspecting Table 1, a typical bridge is a four span, four cell box girder, rigid frame structure, constructed of lightweight concrete. The foundation system consists of concrete pad footings poured on timber piles. Plan, elevation, and cross section views of the girder are shown in Figures 2 and 3. Of the three six foot diameter columns that support the box girder, the center column is rigidly connected to the footing at the lower end, and the girder at the upper ends. The two columns adjacent to the center one are hinged at their bases and rigidly connected to the girder at their upper ends. The ends of the girder are supported on the abutments by rocker shoes which, by design, allow expansion and contraction to occur.

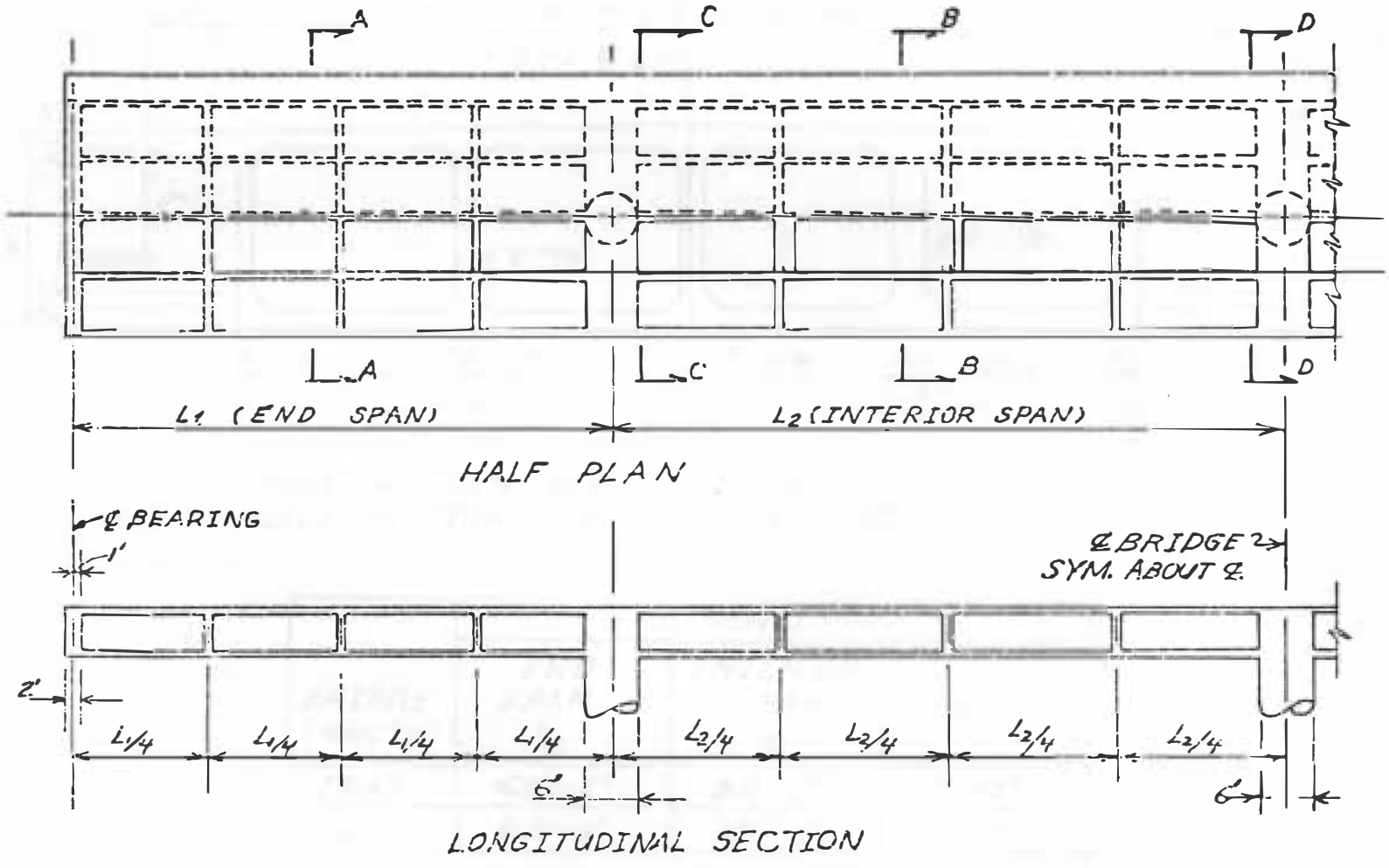

Figure 2 Girder Plan View and Longitudinal Section.

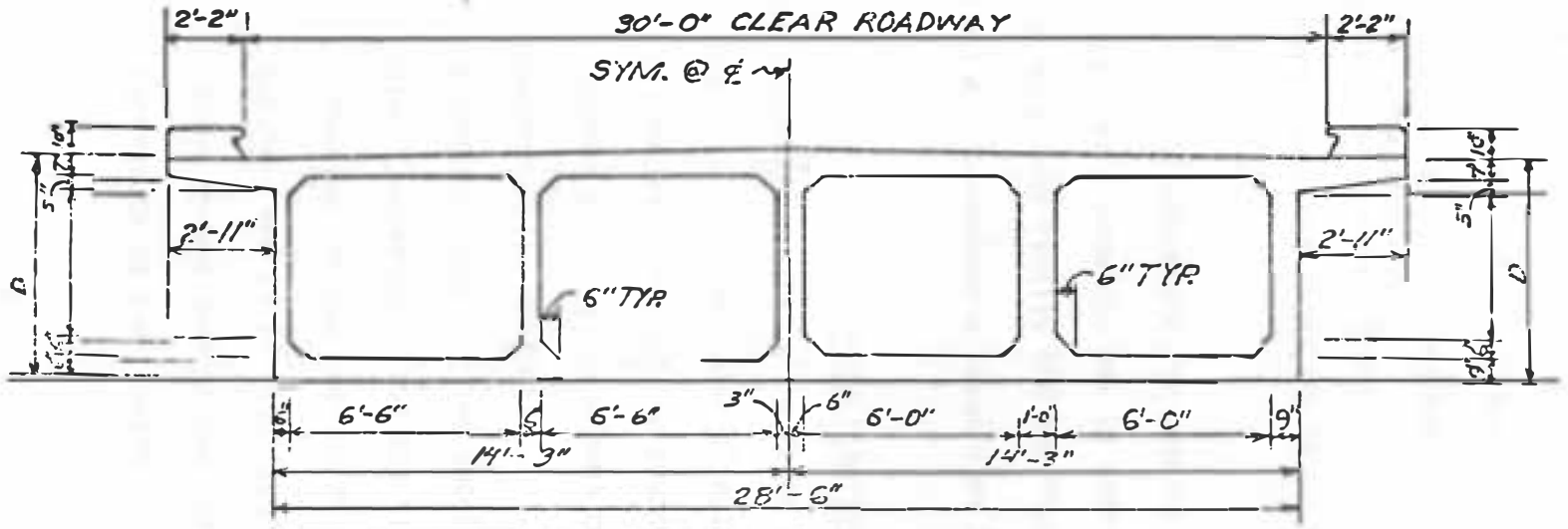

BRIDGE LENGTH	DIMENSIONS		
	END SPAN L_1	INTERIOR SPAN L_2	D
293'	64'-0"	80'-0"	5'-0"
365'	80'-0"	100'-0"	6'-3"

Figure 3 Girder Cross Section, plus Span and Girder Depth Dimensions.

The concrete in the box girder is lightweight concrete which was specified to have a 28 day compressive strength of 4000 lb/in^2. The concrete in the columns and footings is normal weight concrete with a specified 28 day compressive strength of 4000 lb/in^2. Grade 40 steel having a minimum yield point of 40,000 lb/in^2 was specified for the steel reinforcement.

The general procedure for construction of the girders as specified in the engineer's drawings was to pour the bottom flange of the girder, then the webs, and finally the top flange. Seven separate pours were specified with a minimum elapsed time between pours of 72 hours.

Project Outline

The study was conducted in three phases.

1. An inspection was made of each structure.
2. A computer model of the abutment was developed to determine whether or not the abutment movement could be reasonably expected of the design.
3. A computer model of the superstructure was developed to determine a) whether or not the design loadings would cause overstressing in the regions of the girder where the cracking had occurred and b) if significant forces were being transmitted to the girder through the closed expansion devices which could contribute to the cracking.

DATA AND METHODS

Field Observations

The observations were performed on three separate dates. The high temperature on each of those dates was between 95 and 100 degrees fahrenheit. At those temperatures the structures would have been in a state of near maximum expansion.

No record of 'as built' dimensions could be found; therefore three field measurements were required for each side of every abutment to estimate the horizontal translations of the abutments. The distance from the abutment backwall to the center of the rocker shoe anchor bolts was called measurement "A". Measurement "B" was taken as the distance between the end of the girder and the abutment backwall. Measurement "C" was taken from the end of the girder to the center of bearing between the girder and the shoe. A, B, and C are shown in a sketch at the bottom of Table 2.

An estimate of the rotation of the abutment backwall was obtained by measuring the amount by which the wall was out of plumb when compared to a four foot carpenters level. With the level held vertically and one end touching the wall, the gap between the wall and the level at the opposite end was measured. The length of the gap divided by the length of the level yields an estimate of the angle of rotation of the backwall.

A,B,C, and rotation were measured on both sides of the girder at each abutment. The average measurement between the two sides of the girder at each abutment is given in Table 2.

Table 2 Averages of Measurements taken at the Left and Right Sides of the Abutments During the Bridge Inspections.[3]

Bridge No.	Abutment No. 1				Abutment No. 5			
	A[1] in.	B[1] in.	C[1] in.	R[2] rad.	A[1] in.	B[1]	C[1] in.	R[2] rad.
50 180 189	17.44	3.81	11.56	0.0	17.56	3.69	11.44	0.0
50 178 190	19.88	6.19	12.31	0.0	19.75	6.06	11.81	-0.0039
42 066 006	18.69	4.50	11.50	-0.0026	19.12	5.44	11.69	-0.0026
42 067 006	19.56	5.00	11.88	+0.0078	19.56	5.00	12.31	+0.0078
42 065 141	19.90	6.12	11.75	+0.0104	19.12	6.38	11.62	+0.0208
64 008 205	19.56	6.31	12.00	+0.0156	20.38	6.38	12.62	+0.0208
64 079 287	19.50	7.00	11.62	-0.0052	19.44	6.50	12.00	0.0
64 080 296	19.56	5.06	11.69	0.0	19.50	5.56	11.75	+0.0026
64 100 315	19.56	5.75	12.25	0.0	20.00	6.25	12.81	+0.0039
64 115 330	19.19	5.75	11.19	0.0	19.62	5.50	10.94	-0.0104
64 120 336	19.25	4.94	11.75	-0.0104	18.94	4.19	11.69	-0.0247
64 140 355	19.06	5.00	11.62	0.0[4]	18.81	4.56	11.31	-0.0326
64 149 367	19.31	6.94	11.31	-0.0208	19.44	6.75	12.12	-0.0234

Note 1: A, B, and C defined on the sketch at the right.
Note 2: R, rotation, positive counterclockwise. coordinate system shown at the right.
Note 3: Temperatures in the upper 90°F on the day of the Inspections.
Note 4: -0.0130, Rt. side, +0.0130, Lt. side.

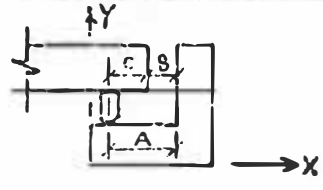

Sketches were made of the crack patterns at the abutments and the interior bents on each side of the girder. Sketching was chosen as the most efficient and accurate means available to the researchers for recording the crack data for study at a later time. Binoculars were used to observe the interior bents. Typical observed crack patterns are shown in Figure 4. The sketches were later reviewed and the cracks were categorized as to number, and whether they occurred in the upper third, the middle third, or the lower third of the web. In order for a crack to be tabulated it had to be judged to have progressed at least half-way through the diaphragm at that particular bent or abutment. The results of this analysis are presented in Table 3. Information is listed for each bridge as well as totals at abutments, totals at interior bents, and totals at each bridge. The numbers in parenthesis indicate the number of cracks out of the total that occurred in the construction joints between the flanges and the web.

A considerable amount of erosion of the berm at the toe of the abutment was observed at several of the bridges. The berm would tend to develop passive earth pressure in resistance to the abutment translations which had occurred. The berm configuration is shown in Figure 5. A visual estimate of the erosion was made to determine the significance of the erosion on the abutment movement. The estimated reduction in passive soil pressure at each abutment based on the design berm configuration is given in Table 4. It should be noted that these values are very crude indicators, and they are probably accurate only in a relative sense.

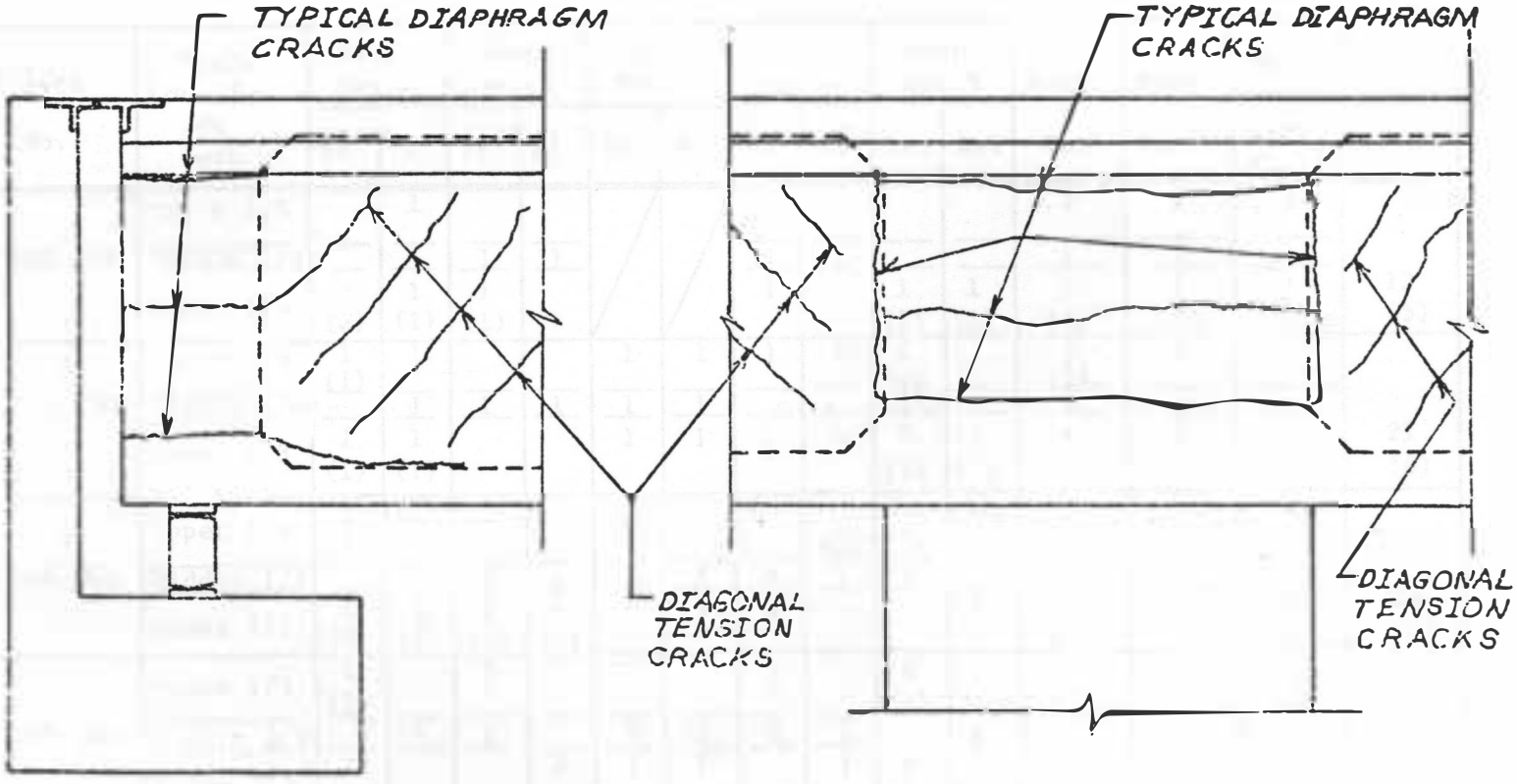

Figure 4 Typical Observed Crack Patterns at Abutments and Bents Based on Bridge Inspection Data August 7, 1980.

Table 3 Crack Summary by Bridge.*

Bridge No.	Crack Location on web	Abut. No. 1		Bent No. 2		Bent No. 3		Bent No. 4		Abut. No. 5		Abut. Tot.	Bent Tot.	Abut. + Bent Tot.	Tot. Each Brdg.
		Lt.	Rt.	Lt.	Rt.	Lt.	Rt.	Lt.	Rt.	Lt.	Rt.				
50 180 189	Upper 1/3		1					1				1	1	2	
	Middle 1/3		1	1	1				1			1	3	4	
	Lower 1/3	1 (1)	1 (1)	1 (1)				1	1	1 (1)	1 (1)	4 (4)	3 (1)	7 (5)	13 (5)
50 178 190	Upper 1/3	1 (1)	1			1	1	1	1	1 (1)		3 (2)	4	7 (2)	
	Middle 1/3		1	1	1	1	1			1		2	4	6	
	Lower 1/3	1 (1)	1 (1)			1	1	1	1	1 (1)	1 (1)	4 (4)	4	8 (4)	21 (6)
42 066 006	Upper 1/3	1 (1)							1 (1)	1 (1)	1 (1)	3 (3)	1 (1)	4 (4)	
	Middle 1/3		1	2	1	1	1	1	1	1		2	7	9	
	Lower 1/3	1 (1)	1 (1)	1 (1)	2 (1)	1	1	1	1		1	3 (2)	7 (2)	10 (4)	23 (8)
42 067 006	Upper 1/3	1 (1)		1				1	1	1 (1)		2 (2)	3	5 (2)	
	Middle 1/3		1	1		1	1	1	1		1	2	5	7	
	Lower 1/3	1 (1)			1	1	1		1	1 (1)	1 (1)	3 (3)	4	7 (3)	19 (5)
42 065 141	Upper 1/3		1 (1)	2 (1)	1	1		1		1 (1)	1 (1)	3 (3)	5 (1)	8 (4)	
	Middle 1/3				1	1	1	1	1	1	1	2	5	7	
	Lower 1/3		1	2 (1)	1	1	2	1	1 (1)	1 (1)	1 (1)	3 (2)	8 (2)	11 (4)	26 (8)

*Numbers in parenthesis are the number of cracks out of the total observed that are located at the junction between the web and flange.

Table 3 Crack Summary by Bridge.* (Cont.)

Bridge No.	Crack Location on web	Abut. No. 1		Bent No. 2		Bent No. 3		Bent No. 4		Abut. No. 5		Abut. Tot.	Bent Tot.	Abut. + Bent Tot.	Tot. Each Brdg.
		Lt.	Rt.	Lt.	Rt.	Lt.	Rt.	Lt.	Rt.	Lt.	Rt.				
64 008 205	Upper 1/3	1 (1)	1 (1)	1	2	1		1 (1)			1 (1)	3 (3)	5 (1)	8 (4)	
	Middle 1/3			1		1		1				0	3	3	
	Lower 1/3	1 (1)	1 (1)		1					1	1 (1)	4 (3)	1	5 (3)	16 (7)
64 070 287	Upper 1/3	1 (1)	1 (1)	1 (1)	1 (1)	1 (1)				1 (1)	1 (1)	4 (4)	3 (3)	7 (7)	
	Middle 1/3			1	1	1	1	1				0	5	5	
	Lower 1/3	1 (1)		1	1 (1)	1	1 (1)	1	1	1 (1)		2 (2)	6 (2)	8 (4)	20 (11)
64 080 296	Upper 1/3	1 (1)	1 (1)		1		1			1 (1)	1 (1)	4 (4)	2	6 (4)	
	Middle 1/3					1		2	1			0	4	4	
	Lower 1/3	1 (1)		1		1	1		1	1 (1)		2 (2)	4	6 (2)	16 (6)
64 100 315	Upper 1/3	1 (1)	1 (1)	1	1				1 (1)	1 (1)	2 (1)	5 (4)	3 (1)	8 (5)	
	Middle 1/3		1		1	1	1	1		1		2	4	6	
	Lower 1/3		1 (1)			1 (1)				1 (1)	1 (1)	3 (3)	1 (1)	4 (4)	18 (9)
64 115 330	Upper 1/3	1 (1)				1				1 (1)	1 (1)	3 (3)	1	4 (3)	
	Middle 1/3				1		1					0	2	2	
	Lower 1/3	1 (1)	1 (1)	2	1	1		1 (1)	1	1 (1)	1 (1)	4 (4)	6 (1)	10 (5)	16 (8)

*Numbers in parenthesis are the number of cracks out of the total observed that are located at the junction between the web and flange.

Table 3 Crack Summary by Bridge.* (Cont.)

Bridge No.	Crack Location on web	Abut. No. 1		Bent No. 2		Bent No. 3		Bent No. 4		Abut. No. 5		Abut. Tot.	Bent Tot.	Abut. + Bent Tot.	Tot. Each Brdg.
		Lt.	Rt.	Lt.	Rt.	Lt.	Rt.	Lt.	Rt.	Lt.	Rt.				
64 120 336	Upper 1/3	1 (1)	1 (1)		1					1 (1)	1 (1)	4 (4)	1	5 (4)	
	Middle 1/3						1		1		1	1	2	3	
	Lower 1/3	1 (1)	1 (1)	1	2 (1)		1 (1)			1 (1)	1 (1)	4 (4)	4 (2)	8 (6)	16 (10)
64 140 355	Upper 1/3	1 (1)	1 (1)							1 (1)	1 (1)	4 (4)	0	4 (4)	
	Middle 1/3						1	1				0	2	2	
	Lower 1/3	1 (1)	1			1			1	1 (1)		3 (2)	2	5 (2)	11 (6)
64 149 367	Upper 1/3	1 (1)	1 (1)							1 (1)	2 (1)	5 (4)	0	5 (4)	
	Middle 1/3				1		1					0	2	2	
	Lower 1/3	1 (1)		1		1			1	1 (1)	1 (1)	3 (3)	3	6 (3)	13 (7)
	Upper 1/3	11 (11)	10 (8)	6 (2)	7 (1)	5 (1)	2	5 (1)	4 (2)	11 (11)	12 (10)	44 (40)	29 (7)	73 (47)	
	Middle 1/3	0	5	7	8	8	10	9	6	4	3	12	48	60	
	Lower 1/3	11 (11)	9 (7)	10 (3)	9 (3)	10 (1)	8 (2)	6 (1)	10 (1)	12 (11)	10 (9)	42 (38)	53 (11)	95 (49)	
	Totals	22 (22)	24 (15)	23 (5)	24 (4)	23 (2)	20 (2)	20 (2)	20 (3)	27 (22)	25 (19)	98 (78)	130 (18)	228 (96)	

*Numbers in parenthesis are the number of cracks out of the total observed that are located at the junction between the web and flange.

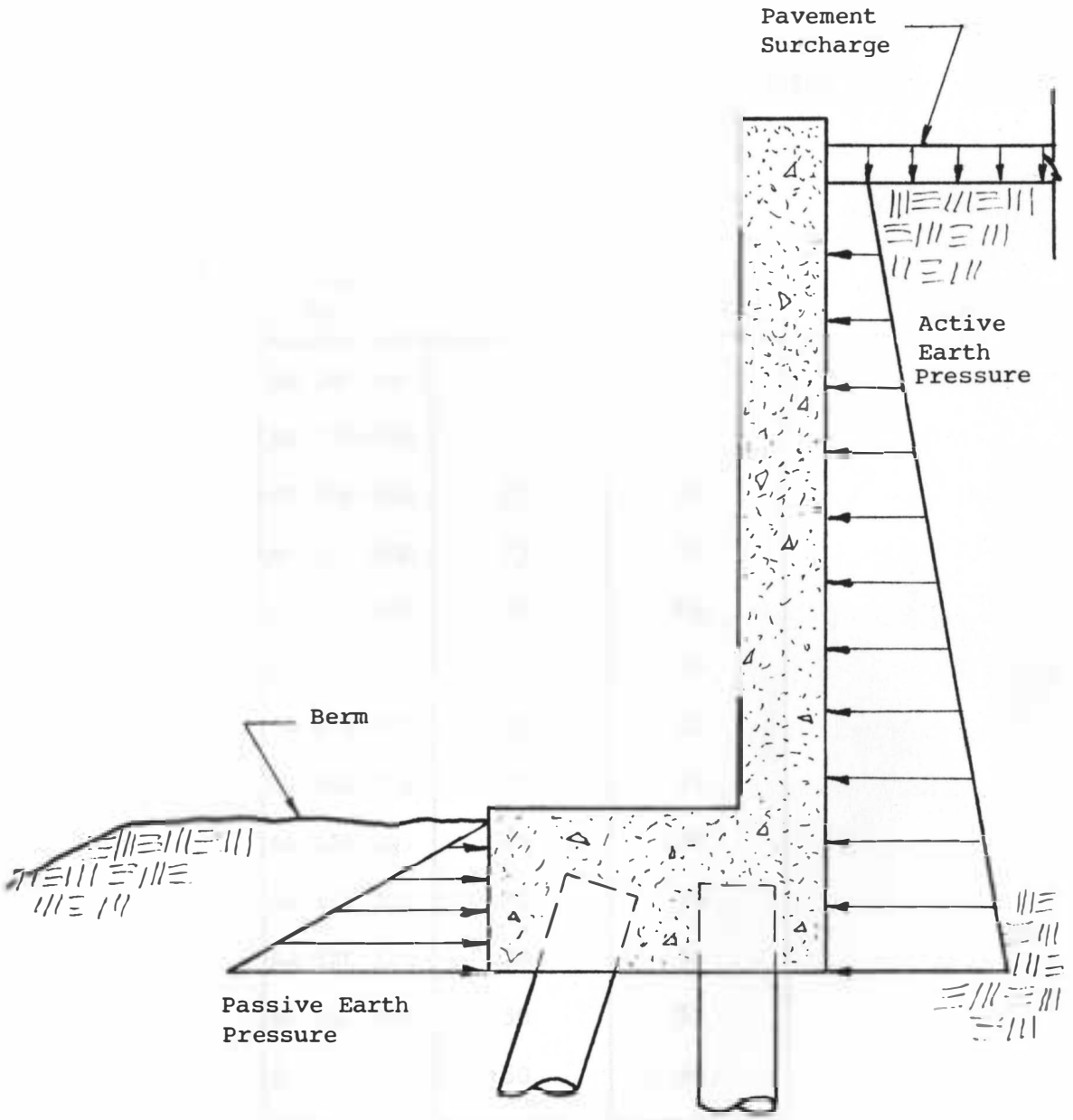

Figure 5 Abutment and Berm Configuration Showing Earth Pressure Diagrams.

Table 4 Visual Estimate of the Percent Reduction in Passive Soil Pressure.

Bridge No.	Abutment No. 1	Abutment No. 5
50 180 189	25	20
50 178 190	15	15
42 066 006	15	35
42 067 006	15	10
42 065 141	20	20
64 008 205	20	20
64 070 287	40	10
64 080 296	55	55
64 100 315	65	100
64 115 330	70	10
64 120 336	30	30
64 140 355	50	55
64 149 367	50	50

Elevation measurements were taken at each bent and each abutment along the bridge centerline on nine of the bridges. Again no record of 'as built' elevatons could be found; therefore the data collected could be used only to show relative elevations.

Abutment Analysis

The objective of the abutment analysis was to determine what movements the abutment would be likely to undergo when subjected to a loading that could reasonably be expected to occur. A further objective of this analysis was to determine if the abutment movements observed could be expected from the way the abutment was designed. If not, possibly there were other factors affecting the abutments that were also affecting the behavior of the column footings.

A computer model of the abutment of the four span bridge with end spans of 80 feet and middle spans of 100 feet was developed. The geometry of the abutment is given in Figure 6. The forces acting on the abutment are the end reaction of the girder, the dead weight of the abutment, and the soil pressure loading. A diagram of the soil pressure loading is shown in Figure 5.

The horizontal loading on the backwall of the abutment was assumed to be the active soil pressure loading and the surcharge loading due to the roadway pavement. Rankine's earth pressure theory was used to determine the soil pressure (1). The equivalent fluid weight, γ_f, can be expressed as

$$\gamma_f = K_A \gamma \qquad (1)$$

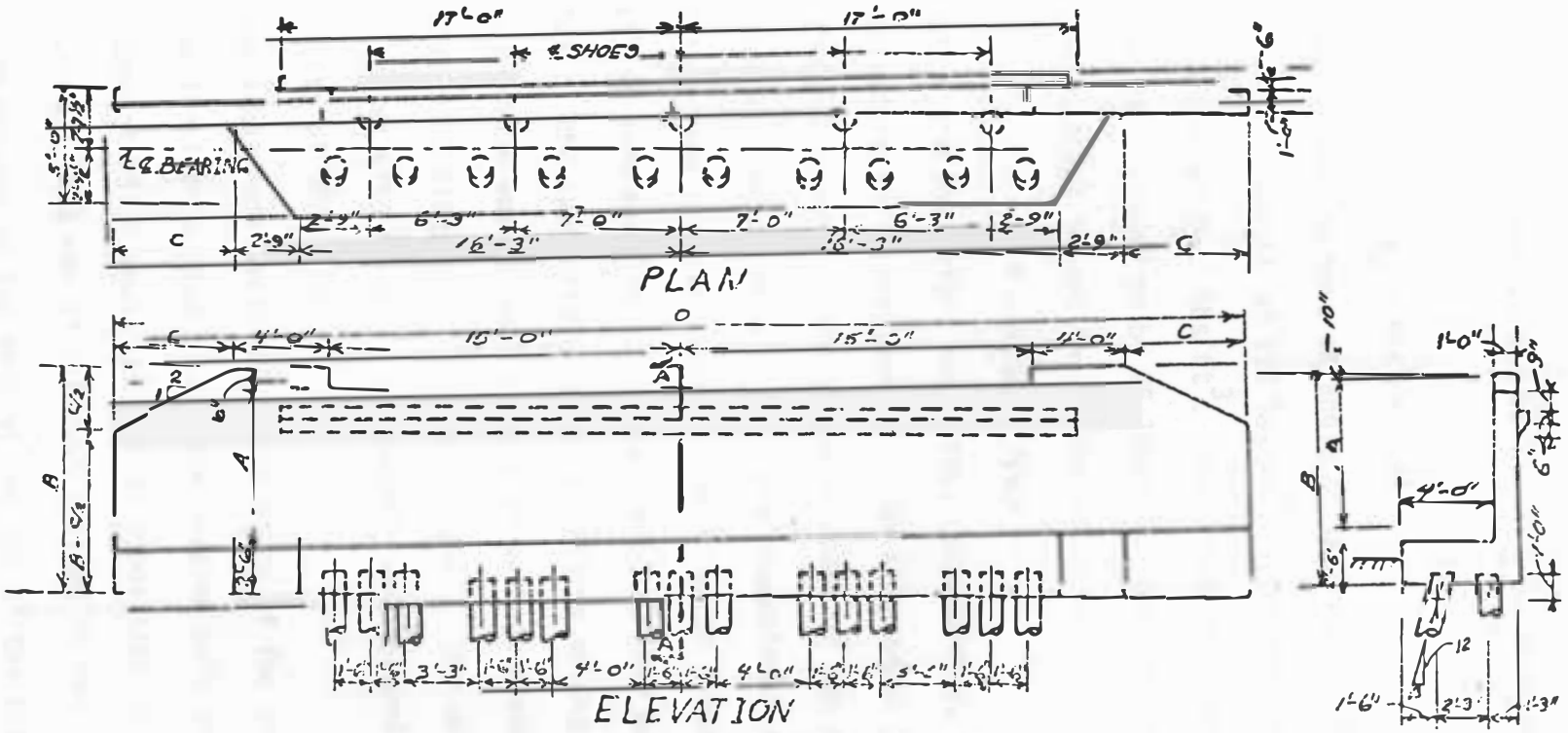

BRIDGE LENGTH	DIMENSIONS				
	A	B	B-C/2	C	O
293'	6'-2½"	9'-6½"	6'-11"	5'-3"	48'-6"
365'	7'-5½"	10'-9½"	7'-6½"	6'-6"	51'-0"

Figure 6 Abutment Geometry

where γ is the unit weight of the soil and K_A is the coefficient of active earth pressure.

$$K_A = \tan^2(45-\tfrac{1}{2}\phi) \qquad (2)$$

The soil was assumed to have an angle of internal friction, ϕ, of 30 degrees and a unit weight of 110 lbs/ft^3. This results in an equivalent fluid unit weight of 36.7 lbs/ft^3. The surcharge loading, q , due to the pavement was assumed to be 75 lbs/ft^2. The total horizontal force pushing the abutment toward the girder would be

$$P = K_A qhw + \tfrac{1}{2}\gamma_f h^2 w \qquad (3)$$

where h and w are the height and width, respectively, of the abutment. For the structure being analyzed, P = 135 kilopounds (Kips).

In the development of the computer model of the abutment the three dimensional problem was reduced to a two dimensional one. The geometry of the plane frame computer model is detailed in Figure 7. Although the timber piling were modeled as single elements, they were assumed to have properties of the appropriate number of piling acting in parallel. An individual piling was assumed to have an average diameter of 12 inches and a modulus of elasticity of 1500 Kips/in^2. The abutment sections were modeled as wide beams. The concrete was assumed to have a modulus of elasticity of 3600 Kips/in^2.

Three areas were explored in the study of the behavior of the abutment. The first area studied was the passive soil pressure at the toe of the abutment which would develop in opposition to the movements which have occurred. This was of interest because it had been observed that significant erosion of the berm at the toe of the abutment had taken

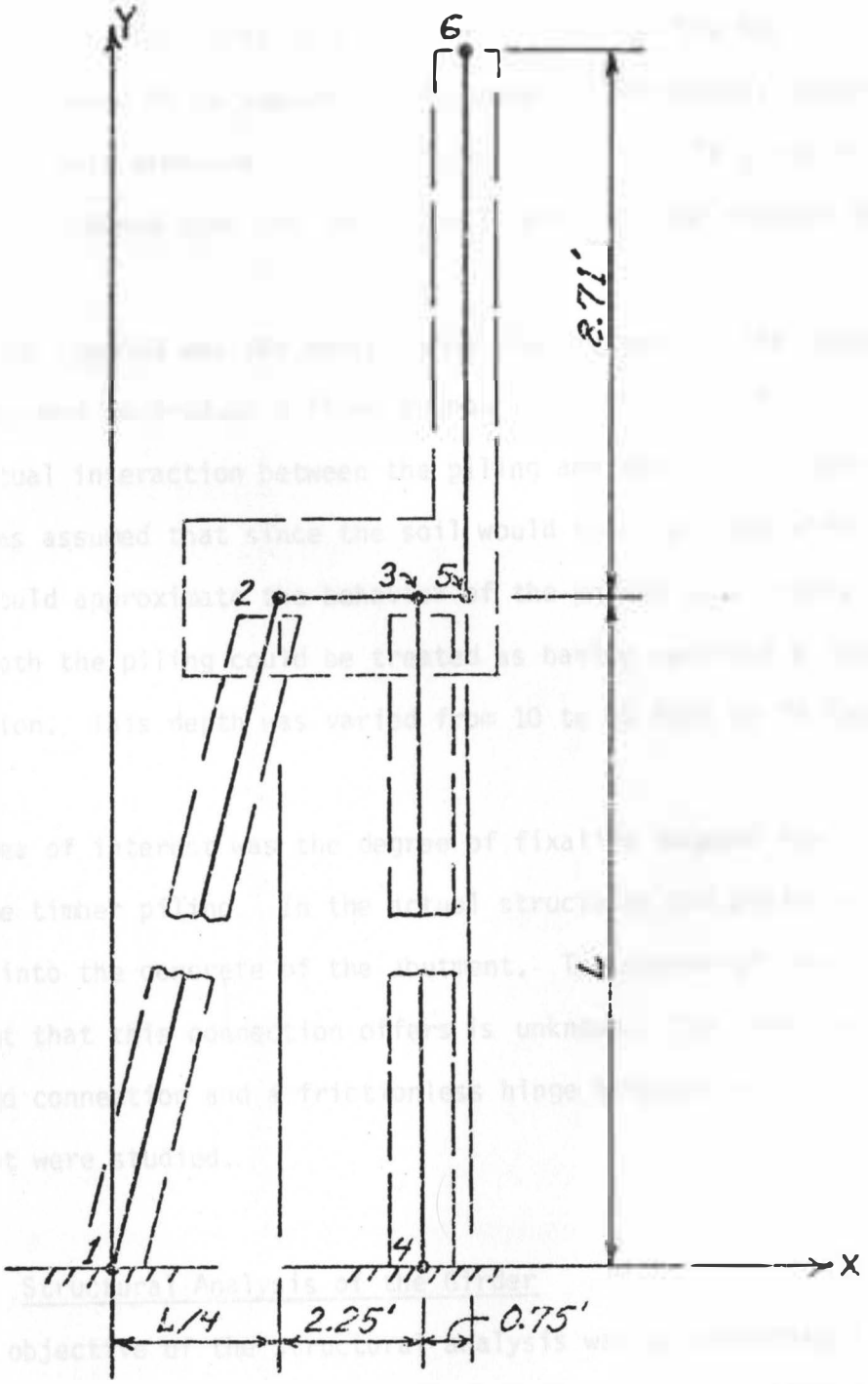

Figure 7 Geometry of the Plane Frame Computer Model Used to Analyze the Abutment.

place. To see what effect this might have on the abutment, two limiting cases were studied. In the first case passive pressure on the toe of the abutment was assumed to be adequate to balance the horizontal component of the active soil pressure. The active soil pressure is given by equation 3. In the second case the passive soil pressure was reduced to zero.

A second area studied was the depth below the abutment of the plane that could be assumed to produce a fixed boundary condition for the piling. The actual interaction between the piling and the soil is complicated. It was assumed that since the soil would tend to creep with time that one could approximate the behavior of the piling by assuming that at some depth the piling could be treated as having achieved a fixed boundary condition. This depth was varied from 10 to 40 feet in 10 foot increments.

A third area of interest was the degree of fixation between the abutment and the timber piling. In the actual structures the piling extends one foot into the concrete of the abutment. The degree of rotational restraint that this connection offers is unknown. The limiting cases of a rigid connection and a frictionless hinge between the piling and the abutment were studied.

Structural Analysis of the Girder

The first objective of the structural analysis was to determine if the design of the structures is adequate with respect to the specified loadings in the regions of the girder where cracking has occurred. The second objective was to determine whether or not significant forces could

be transmitted to the girder through the closed expansion devices which could contribute to the cracking.

As can be seen by referring to Table 1, four distinct configurations of span numbers, span lengths, and deck widths exist in the group of bridges considered in this study. The analysis concentrated on those structures having four spans and decks 34.3 feet wide. Eleven of the fifteen structures are included within this category. The cracking observed in those structures which were not included in the analysis could not be distinquished from the cracking observed in the structures which were included; therefore, the development of two more computer models was not warranted.

The cross sectional properties required for the analysis were based upon the uncracked concrete area with no allowance for reinforcing steel. It is reasonable to use the uncracked section properties in the analysis since the primary concern is for the relative stiffnesses of the members (2). Figure 3 gives the general configurations of the cross sections. The area of the curb above the level of the roadway surface was neglected.

The Computer Program

Analysis of the bridge superstructure was performed with the aid of the Structural Design Language (STRUDL) computer program. STRUDL is a general, high level program developed at the Massachusetts Institute of Technology for the purpose of solving a wide range of structural engineering problems (3). The version implemented on the IBM 370/148 computer at South Dakota State University is STRUDL-II.

The analysis portion of the program is based on the stiffness method of analysis (4) and is applicable to any structure that can be modeled

using beam type elements. The stiffness analysis assumes small displacements, conservative forces, and linear, elastic behavior. First order effects of axial, torsional, and bending distortions can be considered for the following types of loads: concentrated or distributed moments and forces; temperature gradients across the depths of members; uniform temperature changes; and axial, shear, and rotational displacements. The resulting forces, moments, displacements, and rotations will be determined for any point on the structure which the programmer has specified.

The structure was modeled as a two dimensional frame. The details of the frame used are given in Figure 8. For a frame analysis using STRUDL, beams and columns are idealized as line elements which connect into specified joints. Appropriate cross section and material properties are assigned to each line element.

The box girder is nonprismatic[1] adjacent to the interior bents. The thickness of the webs and bottom flange are tapered linearly from each face of the interior supports for a distance equal to one quarter of the span length. The remaining portions of the girder are prismatic. The nonprismatic nature of the girder can be seen by referring back to Figures 2 and 3. Each of the nonprismatic portions of the girder was modeled by dividing the nonprismatic portion into three prismatic segments. The increased cross section near the interior bents was shown to cause only a minimal increase in stiffness when compared to a prismatic model of the girder.

---

[1]Nonprismatic is defined in this case as a beam of varying cross section.

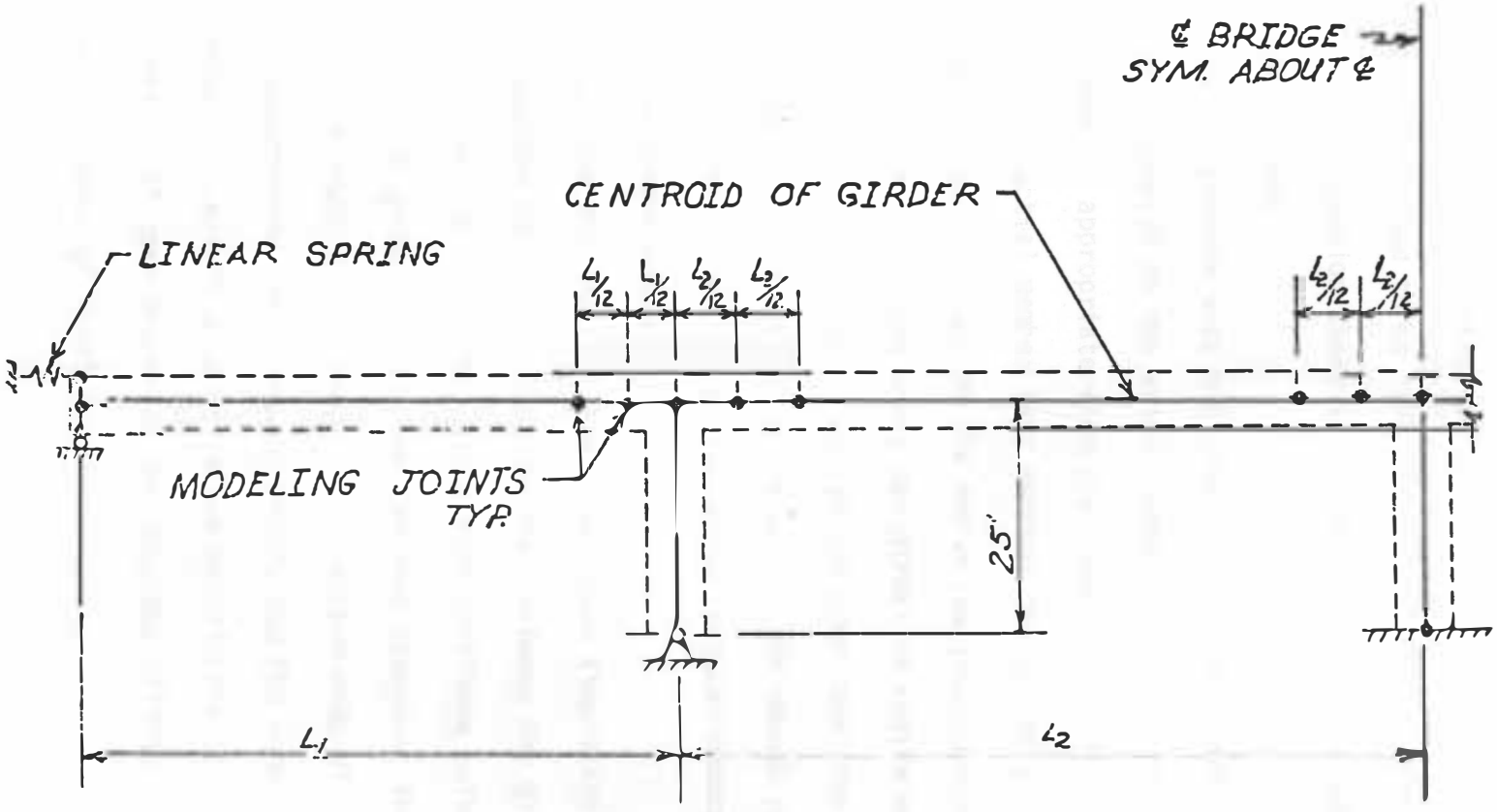

Figure 8 Detail of the Structural Model used in the Computer Analysis of the Bridges.

Consistent with design details, the center column of the bridge was assumed to be completely restrained at its lower end, and the two remaining columns were assumed to be free to rotate but not translate at their lower ends. The expansion shoes at the abutments were assumed to prevent only vertical motion.

The computer program uses one dimensional line elements which coincide with the centroids of the actual members to describe the structure. The line element is appropriate when the lines of action for the support conditions of the actual member pass through the centroid of the member. However, with a situation such as the one at the interface between the abutment and the end of the girder where the girder is restrained vertically at its underside and horizontally at its top edge, the line element with a support node at its end should not be used. The reason being that the horizontal restraint at the top of the girder induces moment into the girder when the girder expands.

To account for the depth of the girder when simulating the condition of closed expansion devices at the interface between the girder and the abutments, two vertical elements having high stiffness values were added to each end of the girder model. The combined length of the two elements was equal to the depth of the girder. The bottom ends of the lower elements were supported by the expansion shoes, and the upper ends of the upper elements were elestically retrained in only the horizontal direction. For the condition of open expansion devices, the stiffness value for the elastic restraint was set equal to zero.

Joints are located at the points of intersection of the member centroids; however, STRUDL allows the programmer to specify the size of any joint, the result being that the length of the member will be decreased by the size of the joint when the stiffness of the member is computed. This command was used to incorporate the comparatively high stiffness of the solid diaphragm over each column.

Influence coefficients were determined by applying the Muller-Breslau principle (5). For this, the model was modified to include joints along the girder at intervals which did not exceed one-tenth of the maximum span length. The added joints were needed only to obtain the deflected shape of the girder, and they did not influence the results of the analysis.

Loading Cases Studied

The loading cases for which the structures were analyzed were dead load, live load, live load plus impact, thermal stresses, shrinkage, support settlements, and abutment earth pressure. Included in the dead load were railings, curbs, overlays, forms left in place, girder weight, and the transverse girder diaphragms. The concrete was assumed to weigh 110 pounds per cubic foot. The H20-44 lane load and the HS20-44 standard truck load from the American Association of State Highway and Transportation Officials (AASHTO) specifications (6) were used in the live load analysis. Dynamic impact effects were taken as 25 percent of the live load. Thermal effects were calculated for a uniform temperature increase of $35^{o}F$ and a decrease of $45^{o}F$ as given by the AASHTO specifications. The effects of a temperature gradient of $-15^{o}F$ from the top of the girder to the bottom were also calculated. Uniform concrete shrinkage strain of 0.0008 was assumed (7). The forces developed by one or both abutments

settling one-tenth of a foot were calculated. A derivation of the abutment earth pressure loading case is given in the following section.

The loading cases were applied individually to the structure and combined for analysis as required by Table 1.2.22 of the AASHTO specifications.

Abutment Earth Pressure Model

The model for determining the magnitude of the loads transmitted to the girder by the abutment was derived from the Rankine earth pressure theory. The basic assumptions used to develop the model were that prior to significant thermal expansion the abutment was resting against the girder, and the soil behind the abutment was in an active pressure state. When the girder expands, the soil pressure against the abutment increases as the pressure state in the soil moves toward the passive pressure condition.

These assumptions dictate a constant force applied to the girder due to the active soil pressure state and an increasing force caused by the expansion of the girder. An estimate of the constant force was arrived at by assuming that the backwall of the abutment behaves as a simple beam resting against the girder at the location of the expansion device and hinged at its lower edge. With the active earth pressure condition applied, the reaction at the expansion joint, R_A, was determined by summing the moments about the lower edge.

$$R_A = \tfrac{1}{2} q K_A h w_1 + \frac{K_A \gamma h^2 w_2}{6} \qquad (4)$$

where w_1 is the width of the roadway and w_2 is the width of the abutment.

The first term on the right-hand side of the equation is the reaction due to the surcharge applied by the roadway surface. The second term is the reaction due to the active soil pressure.

The increase in force transmitted to the girder due to expansion of the girder was modeled by a horizontal spring with an appropriate stiffness constant. The spring was attached to the girder model at the location of the expansion device. A derivation of the stiffness constant for the ficticious spring follows.

As for the active pressure case, the backwall was assumed to behave like a simple beam. The reaction at the expansion device was determined for the passive earth pressure case in the same way that R_A was determined above.

$$R_P = \tfrac{1}{2}qK_P h w_1 + \frac{\tfrac{1}{2} K_P h^2 w_2}{3} \tag{5}$$

K_P is the coefficient of passive earth pressure.

$$K_P = \tan^2 (45 + \tfrac{1}{2}\phi)$$

A stiffness constant can be defined as the increment of force required to maintain equalibrium for each unit of displacement; therefore, the appropriate stiffness for the horizontal spring is

$$K_S = \frac{R_P - R_A}{d_A + d_P} \tag{6}$$

where d_A and d_P are the displacements at the top of the backwall which are required to develop the full active and passive earth pressures, respectively. The displacements d_A and d_P can be expressed in terms of the angle of rotation of the backwall, α_A or α_P and the height of the backwall.

$$d_A = \alpha_A h \tag{7}$$

$$d_P = \alpha_P h$$

Substitution of equations 4, 5, and 7 into the equation 6 gives

$$K_S = \frac{(K_P - K_A)(3qw_1 + hw_2)}{6(\alpha_A + \alpha_P)} \tag{8}$$

With $\phi = 30^o$, $\gamma = 110$ lbs/ft^3, $q = 75$ lbs/ft^2, $\alpha_A = 0.00125$, $\alpha_P = 0.00750$, $w_1 = 30$ ft, $w_2 = 48.5$ ft, and $h = 8.708$ ft, the constant force is 32.66 kips by equation 5, and the linear spring constant is 225.2 kips/inch by equation 8. The rotations α_A and α_P are for cohesionless soil of medium density (1).

A uniform temperature increase of 70^oF was applied to the structure to determine the maximum abutment earth pressure loads acting on the girder. The active earth pressure condition was assumed to be present when the girder was nearly at its minimum length which occurs when the temperature decrease of 45^oF is acting on the girder. Any expansion beyond the minimum length causes an increase in the soil pressure. The maximum girder length occurs when the 35^oF temperature increase is acting on the girder. Thus, the total increase in temperature beyond the point where the increase in earth pressure begins is roughly 70^oF.

RESULTS AND DISCUSSION

Results of the Inspections

Estimated rotations and horizontal translations at each abutment are shown in Table 5. In order to establish the original distance between the abutment backwall and the end of the girder, dimension A was assumed to equal the sum of dimensions B and C at the time of construction. (A, B, and C are shown in the diagram of Table 2.) This assumes that the expansion shoes and the abutment backwall were originally plumb. If this assumption is adopted, the translation (X_t) can be calculated as follows:

$$X_t = (B + C) - A.$$

A negative value of X_t indicates an apparent translation of the abutment toward the girder. A negative rotation indicates that the top of the abutment is leaning away from the girder.

The maximum translation was -3.2 inches, the minimum translation was -0.6 inches. The mean translation was -1.94 inches with a standard deviation of 0.78 inches. The abutment rotations ranged between -0.0326 radians and +0.0208 radians with an average and standard deviation of -0.0018 radians and 0.0127 radians respectively.

When viewing the results of the abutment translation and rotation the following points should be noted. The amount of abutment translation or rotation towards the girder is limited by either the opening in the expansion device, or the distance from the abutment backwall to the end of the concrete curb on the bridge at the time of construction. For a temperature of 70 degrees fahrenheit the design openning at the expansion

Table 5 Estimated Abutment Translation and Rotation

Bridge No.	Abutment No. 1			Abutment No. 5		
	X_t[1] in.	Br. Shoes Leaning as noted[2]. in.	Rot. R rad.[3] (deg.)	X_t[1] in.	Br. Shoes Leaning as noted[2]. in.	Rot. R rad.[3] (deg.)
50 180 189	-2.06	2.5 Lt. side	0.0	-2.44	2.5 Lt. side	0.0
50 178 190	-1.37		0.0	-1.87		-0.0039 (-0.22)
42 066 006	-2.69		-0.0026 (-0.15)	-2.00		-0.0026 (-0.15)
42 067 006	-2.69		+0.0078 (+0.45)	-2.25		+0.0078 (+0.45)
42 065 141	-2.02		+0.0104 (+0.60)	-1.12		+0.0208 (+1.19)
64 008 205	-1.25		+0.0156 (+0.89)	-1.38		-0.0208 (-1.19)
64 070 287	-0.88		-0.0052 (-0.30)	-0.94		0.0
64 080 296	-2.81		0.0	-2.19		+0.0026 (+0.15)
64 100 315	-1.56		0.0	-0.94		+0.0039 (+0.22)
64 115 330	-2.25		0.0	-3.19		-0.0104 (-0.60)
64 120 336	-2.56		-0.0104 (-0.60)	-3.06	Leaning severly	-0.0247 (-1.42)
64 140 355	-2.44		0.0	-2.94	2.0 Lt. side	-0.0326 (-1.89)
64 149 367	-1.06		-0.0208 (-1.19)	-0.56		-0.0234 (-1.34)

Note 1: Negative values indicate abutment translation towards the girder.

Note 2: Bridge shoes leaning in expansion the amount tabulated.

Note 3: Positive rotations indicate the abutment is tilted towards the girder.

device was two inches. In almost every case either the expansion device was fully closed or, in cases where the fingers in the expansion device had been cut, the end of the concrete curb was resting against the backwall. It should also be noted when viewing the values of the rotations that the error due to construction tolerances and measurement methods is estimated to be ± 0.005 radians. An angle of 0.005 radians is about 0.25 inches offset from vertical in four feet.

A search for linear association was carried out between the translation and the average daily traffic[1]; the translation and the rotation; and the translation at abutment number 1, and the translation at abutment number 5. Of these, only the last showed notable correlation. A correlation coefficient of 0.73, significant at the 1.0% level based on a sample of size 13, was obtained between the translation at abutments 1 and 5. This indicates that larger than average translations at abutment 1 tend to be associated with larger than average translations at abutment 5. The correlations were essentially zero for the other parameters tested.

Similarly for the rotation data, linear association was sought between the rotation and the average daily traffic; the rotation at abutment 1 and abutment 5; and, as noted above, between the rotation and the translation at an abutment. The results showed essentially zero correlation except between the rotation at abutment 1 and abutment 5 where a correlation coefficient of 0.76 was calculated. It should be noted that although the correlation between the rotation at abutment 1 and the rotation at abutment 5 is nearly equal to the correlation between the

---

[1]Traffic information was supplied by the SDDOT.

translation at abutment 1 and the translation at abutment 5, translations show almost zero correlation with rotations at a given abutment.

An inspection of Table 5 reveals that in every case the translation of the abutment appears to be towards the girder. Also, there is no apparent tendency for the rotation to be toward or away from the girder. The rotational behavior of the abutments is probably explained by soil conditions which vary from bridge to bridge and by the interferences between the girder and the abutment as the abutment movement occurs.

The number of cracks found in an individual girder ranged from a minimum of 11 to a maximum of 26. The average number of cracks was 17.9 and the standard deviation was 4.03. Of the cracks at the abutments, 79 percent were located in the construction joints between the web and the upper or lower flanges of the girder. Of the cracks at the interior bents, only 14 percent were located at the intersection between the web and the flanges. This suggests that the cause of the cracking at the abutments is not necessarily related to the cause of the cracking at the interior bents. No linear association was found between the cracking and the average daily traffic.

All of the structures inspected exhibit diagonal tension cracks adjacent to supports. Such cracks are expected and they appear to be well controlled by the design shear reinforcement.

No linear association was found between the estimated reduction in passive soil pressure given in Table 4 and the abutment translation.

The elevation data was utilized as follows. The assumption was made that the present elevation at the center pier is equal to the design

elevation at that point. Present elevations at the remaining supports were computed from the data and compared to the design elevations. The estimated differential settlements at the bridges for which elevation data were taken can be found in Table 6. This approach assumes also that each bridge was built to the design vertical curve shown on the construction drawings. The actual settlements cannot be verified because it is not known how closely each bridge was built to its design vertical curve; however, the information in Table 6 does suggest that significant relative settlements have occurred at several of the abutments.

Comments from Visual Observations

The observation was made at several of the bridges, especially at the ends of the girders, that segration of the aggregates in the concrete had occurred at the time of pouring. In lightweight concrete, segregation is commonly the result of excessive water content in the mix because the lightweight aggregates will tend to float on the water-cement paste (8). Control of the water content in lightweight concrete is an inherent difficulty due to the high absorptive capacity of lightweight aggregates (7). Excess water in concrete is detrimental since it reduces strength and increases the potential for drying shrinkage (9).

As noted earlier, 79 percent of the cracks at the ends of the girders have occurred in the construction joints between the pours for the web and the top and bottom flanges. A factor which has promoted this cracking is drainage water from the bridge deck which flows through the expansion.

Table 6 Estimated Differential Settlements at Abutments and Bents.

Bridge No.	Abut No. 1 ft. (in.)	Bent No. 2 ft. (in.)	Bent No. 3 ft. (in.)	Bent No. 4 ft. (in.)	Abut No. 5 ft. (in.)
50 180 189	+0.01 (+0.1)	-	**	+0.08 (+1.0)	+0.03 (+0.4)
50 178 190*	-0.05 (-0.6)	0.0	**	+0.01 (+0.1)	-0.09 (-1.1)
42 066 006	-0.09 (-1.1)	+0.03 (+0.4)	**	+0.02 (+0.2)	+0.08 (+1.0)
42 067 006	-0.14 (-1.7)	-0.03 (-0.4)	**	0.0	-0.07 (-0.8)
42 065 141	+0.04 (+0.5)	-0.01 (-0.1)	**	+0.01 (+0.1)	+0.07 (+0.8)
64 070 287*	+0.01 (+0.1)	+0.02 (+0.2)	**	0.0	+0.03 (+0.4)
64 100 315*	-0.40 (-4.8)	-0.07 (-0.8)	**	-0.03 (-0.4)	-0.32 (-3.8)
64 115 330*	-0.24 (-2.9)	-0.05 (-0.6)	**	-0.09 (-1.1)	-0.18 (-2.2)
64 149 367*	-0.29 (-3.5)	-0.03 (-0.4)	**	-0.03 (-0.4)	-0.16 (-1.9)

*Level data taken in inspections of August 7. All other level information obtained from the Department of Transportation.

**Design vertical curve assumed to match existing structure at this point.

device, down the end of the girder, and into the construction joints. When freezing occurs, cracking results. This explanation is also consistent with the lower incidence of construction joint cracking at the interior bents. Drainage from the bridge deck is channelled to the ends of the girder; whereas, the sides of the girder are shielded by the upper flange which extends three feet beyond the sides of the girder.

Results of the Abutment Analysis

The computer models and loadings of the abutment were input and run using the plane frame portion of the STRUDL Program. The primary interest was in the displacements obtained from this program. The results at joint 3 of the model are given in Table 7. Displacements are positive with respect to the coordinate axis shown in Figure 7. Rotations are positive counterclockwise. A plot of the results when the piling are assumed rigidly connected to the abutment are presented in Figure 9.

The results at joint 3 were selected for two reasons. First, the horizontal movement of the joint corresponds to the horizontal movement of the abutment measured in the field; second, it was expected and substantiated in the analysis that the abutment acts essentially as a rigid body. Thus, joints 2, 3, and 5 have equal horizontal displacements, and joints 2, 3, 5, and 6 have equal rotations. The horizontal displacement of joint 6 can be calculated by utilizing the horizontal displacement of joint 3, the rotation of joint 3, and the length of the member between joints 5 and 6.

The observation has been made regarding Table 5 that all of the abutments appear to have translated toward the girder. The results of the

abutment analysis given in Table 7 are in agreement with the observed behavior only when the passive earth pressure at the toe of the abutment is neglected. This conclusion is supported by the fact that no linear association was found between the amount of erosion and the translation at the abutment. It is suspected that the horizontal portion of the berm at the toe of the abutment does not extend far enough from the toe to develop significant passive pressure.

The assumption was made that at some depth below the abutment the piling achieved a fixed end condition. This assumption yielded results which were in agreement with the observed abutment movements as the assumed depth approached 40 feet.

One cannot place a great deal of confidence in the numerical results obtained from the assumed pinned connection between the piling and the abutment because the problem becomes extremely nonlinear under this assumption. However, the results obtained do indicate the general nature of the deflections the abutment would undergo under the assumed hinge condition.

McNulty (10) suggested that 12 inch diameter timber piles should be embedded about two feet into the concrete cap to insure a practically rigid connection. The piling for the abutments were embedded about one foot; therefore, a considerable degree of fixation between the piling and the abutment is probably achieved. The results in Table 7 are in agreement with this conclusion.

The abutment analysis indicates that the movement which the abutments have undergone could reasonably be expected from the geometric configuration of the abutment design. The results do not indicate that unusual

Table 7 Results of the Computer Analysis of the Abutment under Soil Pressure Loading.

Distance L ft.	Piling Rigidly Attached to Abutment				Piling Hinged at Attachment to Abutment			
	Zero Passive Pressure		Passive Pressure Equals Active Pressure		Zero Passive Pressure		Passive Pressure Equals Active Pressure	
	X Displ. Jt. 3 in.	Z Rot. Jt. 3 rad. (deg.)	X Displ. Jt. 3 in.	Z Rot. Jt. 3 rad. (deg.)	X Displ. Jt. 3 in.	Z Rot. Jt. 3 rad. (deg.)	X Displ. Jt. 3 in.	Z Rot. Jt. 3 rad. (deg.)
10	-0.13	-0.0005 (-.03)	+0.17	+0.0011 (+0.06)	-1.05	-0.0094 (-0.54)	+1.52	+0.014 (+0.80)
20	-0.55	-0.0032 (-0.18)	+0.74	+0.0050 (+0.29)	-8.36	-0.077 (-4.41)	+6.34	+ .059 (+3.38)
30	-1.11	-0.0071 (-0.41)	+1.52	+0.0108 (+0.62)	-28.2	-0.260 (-14.9)	+41.2	+0.382 (+21.9)
40	-1.76	-0.0117 (-0.67)	+2.42	+0.0175 (+1.00)	_[2]	_[2]	_[2]	_[2]

Note 1: For definition of L and positive direction of X, see Fig. 3.2. Rotations positive counterclockwise see Fig. 3.7.

Note 2: These values not computed, would require large displacement analysis to obtain solution.

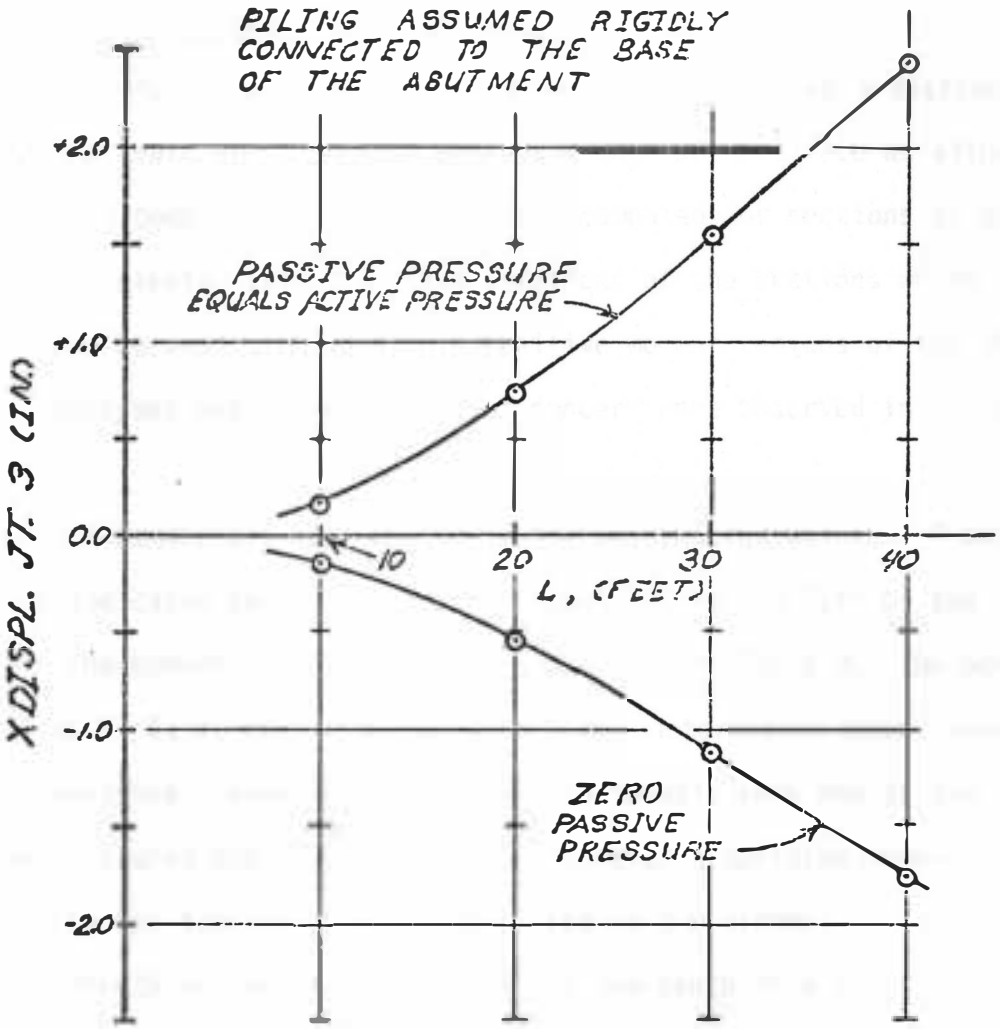

Figure 9 Abutment Translation vs. Depth To Fixed Boundary Condition at the Lower End of the Piling.

soil conditions are present which could be affecting the column footings.

Results of the Structural Analysis of the Girder

Shearing forces were computed for sections located at a distance equal to the depth of the member away from each support face as allowed by the AASHTO code. Bending moments were computed for sections at each face of the interior supports. The locations of the sections which were analyzed can be seen in Figure 10. Positive moment regions of the girder were not analyzed because no cracks of concern were observed in those regions.

Table 8 summarizes the results of the shear calculations. A positive sign indicates an upward vertical resultant to the left of the section. The moment calculations are summarized in Table 9. The moments at sections H, I, J, and K were used only for determining shear capacities at those sections; therefore, the live load moments were due to the live loads which caused the maximum shearing forces. A positive moment is one which causes tension at the bottom face of the girder.

The effects of the abutments settling one-tenth of a foot were determined in the analysis but these effects were not included in the analysis of the results. Justification for ignoring settlement effects stems from the fact that the magnitudes of the settlements cannot be firmly established. It is possible that settlements are a factor in the cracking; however, a study by Moulton and Kula (11) suggests that abutment settlements of three inches or more could occur without causing significant damage to the bridge. In that study, damage is considered

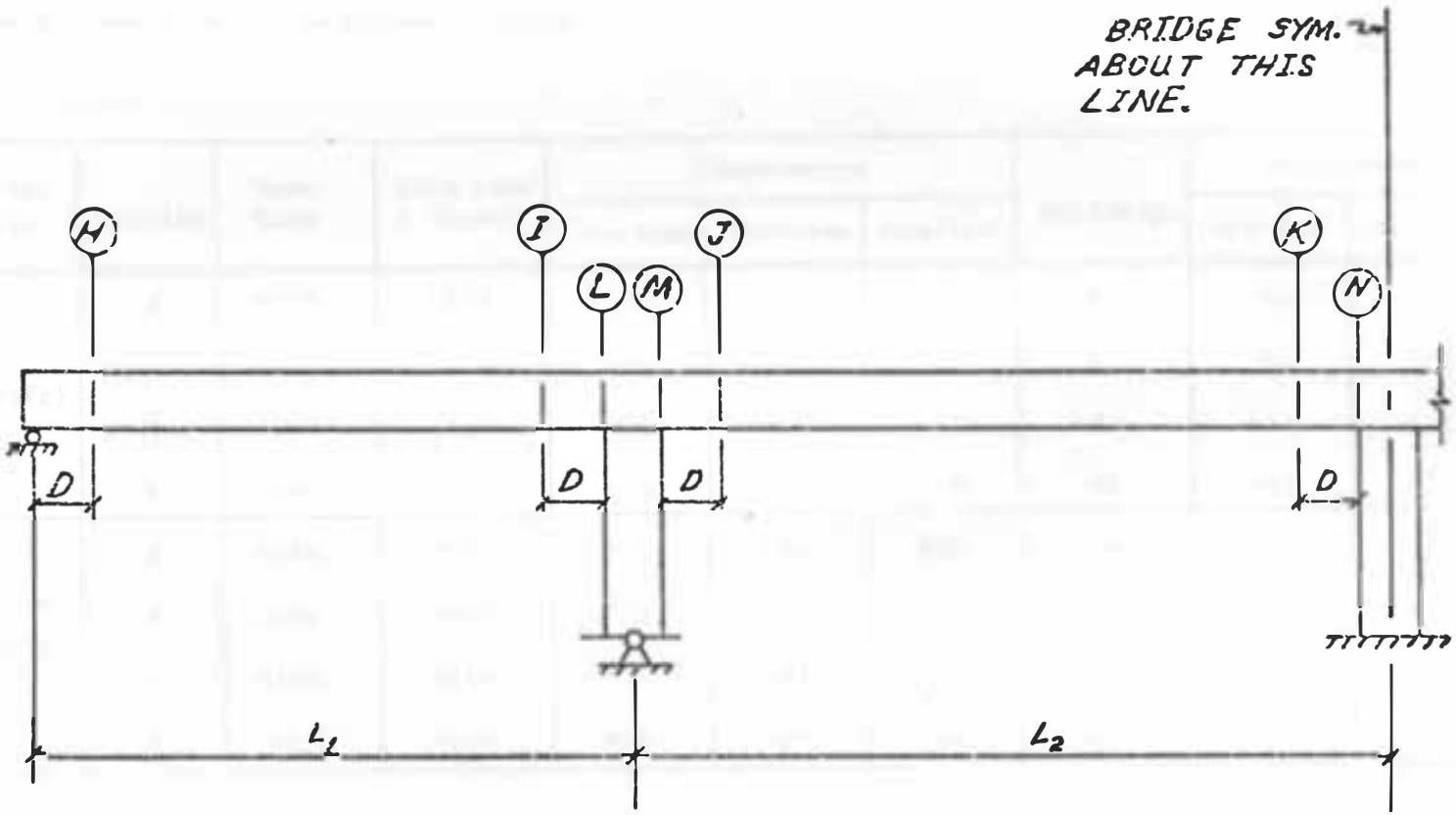

Figure 10 Locations of Analyzed Sections

Table 8 Shear Forces in Kilopound Units

Overall Length	Section	Dead Load	Live Load + Impact	Temperature			Shrinkage	Settlements	
				Increase	Decrease	Gradient		One End	Both Ends
293(ft)	H	+129	+125	+8	-11	+21	-47	-61	-63
	I	-244	-153	+8	-11	+21	-47	-61	-63
	J	+240	+149	+19	-24	-3	-92	+35	+33
	K	-233	-149	+19	-24	-3	-92	+35	+33
365(ft)	H	+170	+132	+11	-14	+22	-58	-50	-51
	I	-324	-157	+11	-14	+22	-58	-50	-51
	J	+313	+154	+21	-27	-4	-104	+31	+30
	K	-312	-154	+21	-27	-4	-104	+31	+30

Table 9 Bending Moments in Foot-Kilopound Units

Overall Length	Section	Dead Load	Live Load + Impact	Temperature			Shrinkage	Settlements	
				Increase	Decrease	Gradient		One End	Both Ends
293(ft)	H	+730	+456*	+42	-54	+106	-233	-303	-312
	I	-2119	-343*	+469	-603	+1189	-2614	-3398	-3499
	J	-2316	-497*	-811	+1043	+1091	+4023	-1547	-1446
	K	-2115	-575*	+390	-501	+870	-1932	+715	+691
	L	-3436	-1302	+510	-657	+1295	-2847	-3701	-3812
	M	-3422	-1472	-891	+1145	+1106	+4419	-1697	-1589
	N	-3381	-1451	+482	-620	+852	-2393	+889	+856
365(ft)	H	+1202	+629*	+68	-193	+140	-365	-311	-320
	I	-3599	-624*	+765	-984	+1579	-4128	-3513	-3639
	J	-3658	-774*	-1143	+1470	+1475	+5694	-1739	-1667
	K	-3619	-765*	+555	-714	+1159	-2767	+767	+807
	L	-5809	-1936	+833	-1071	+1719	-4496	-3826	-3940
	M	-5800	-2168	-1278	+1643	+1499	+6349	-1933	-1859
	N	-5754	-2158	+687	-883	+1111	-3422	+943	+999

*Moment due to loading that causes maximum shear at the section

to be significant if the structural integrity, appearance, or rideability is impaired.

A summary of the results of the abutment earth pressure analysis can be found in Table 10. The effects of the abutment earth pressures were determined to be relatively minor. As can be seen from Table 10, the interior spans are practically unaffected by the earth pressure loading. It is noted that in the interior spans the earth pressure effects tend to reduce the stresses due to the critical loading combination. The maximum forces transmitted through the expansion joints are estimated to be 150 kips and 200 kips for the 293 foot and 365 foot structures, respectively. The compressive stresses in the concrete of the girder due to these forces would not be significant.

The results of the analysis of the loading combinations are summarized in Table 11. The allowable shear and moment calculations were based upon the allowable stress approach (6) (12). Each of the allowable values in Table 11 includes the appropriate stress increase allowed by the AASHTO specifications for the associated loading combination. Three AASHTO loading combinations provided the critical loading cases for the analysis (6). Loading Group I consists of the dead load, the live load configuration which causes the maximum stress at the location being analyzed, and the impact effects of the live load. Group IV loading includes Group I plus shrinkage and temperature effects. Finally, Group V loading includes the dead load, 0.75 times the earth pressure load, temperature effects, and shrinkage effects.[1]

[1]Only those loads which are significant to this analysis have been listed here.

Table 10 Results of the Abutment Earth Pressure Analysis

Overall Length	Section	Active Earth Pressure		Earth Pressure due to Girder Expansion[1]	
		Shear Force (kips)	Bending Moment (ft-kips)	Shear Force (kips)	Bending Moment (ft-kips)
293(ft)	H	-2.0	+72	-7.2	+252
	I	-2.0	-28	-7.2	-102
	J	0.0	-4	-0.2	-14
	K	0.0	+2	-0.2	+6
	L	-2.0	-38	-7.2	-136
	M	0.0	-4	-0.2	-16
	N	0.0	+2	-0.2	+8
365(ft)	H	-2.1	+99	-10.7	+487
	I	-2.1	-39	-10.7	-190
	J	0.0	-6	-0.3	-30
	K	0.0	+3	-0.3	+14
	L	-2.0	-52	-10.7	-256
	M	0.0	-7	-0.3	-35
	N	0.0	+3	-0.3	+15

Note 1: Loading case is active only when temperature increase is active.

Table 11 Summary of the Analysis

Overall Length (ft)	Section	Maximum Shear (kips)	Allowable Shear (kips)	Maximum Moment (ft-kips)	Allowable Moment (ft-kips)	Maximum Allowable
293	H	+254	+287	---	---	0.89
	I	-397	-489	---	---	0.81
	J	+389	+487	---	---	0.81
	K	-501	-517	---	---	0.97
	L	---	---	-3269	-8255	1.00
	M	---	---	+2142	+1750	1.22
	N	---	---	-7845	-8255	0.95
365	H	+302	+350	---	---	0.86
	I	-481	-587	---	---	0.82
	J	+467	+596	---	---	0.78
	K	-601	-637	---	---	0.94
	L	---	---	-13348	-12438	1.07
	M	---	---	+2192	+2674	0.82
	N	---	---	-12217	-12438	0.98

Loading Group I provided the critical case for shear at sections H, I, and J, and Group IV was the critical case for section K. Loading Group IV provided the critical case for moment at sections L and N, but the critical moment at section M is a positive moment occurring under Group V loading.

The right-most column of Table 11 lists the ratios of the maximum forces or moments to the allowable forces or moments. Inspection of this column shows that the only ratios greater than one are at section L of the 365 foot structure and sections L and M in the 293 foot structure. The major contribution to the moments at these sections, aside from the dead loads, is concrete shrinkage. The effects of axial tension have not been included in the moment calculations, but they would reduce the moment capacity at sections M and N. The allowable shear at K has been adjusted as outlined in the AASHTO specifications for the axial tension which would be acting as a result of shrinkage and thermal strains.

In summary three points should be noted. First, it is clear from the results presented that the shrinkage of the concrete has resulted in significant forces that would certainly contribute to the cracking that was observed in the inspections. Second, there exists the possibility of significant settlements which, if they have occurred, again have caused significant forces to develop, particularly at the interior bents. The third point is that the abutments resting against the girder are not likely to cause loads of sufficient magnitude to adversely affect the performance of the bridges.

CONCLUSIONS

Based on the analysis that was carried out, the girder design appears to have been adequate to carry most of the design loads. The exception is the stress induced by concrete shrinkage which causes overstress from an allowable stress viewpoint. The loading transferred to the girder by the abutment when the abutment rests against the girder does not lead to forces that should affect the service life of the structure.

The cracks observed at the interior bents are considered to be caused by the combination of the shear, flexural, and shrinkage stresses that occur at these locations. Shrinkage contributes in two ways. First, the shrinkage in the girders causes significant moments to occur at these locations. Second, shrinkage in the large diaphragm at each bent causes strain that would further contribute to the cracking.

If differential settlements greater than two inches have occurred on bridges 64 100 315, 64 115 330, and 64 149 367 as indicated by the data in Table 6, these bridges are certainly overstressed from an allowable standpoint. Settlement of an abutment would cause an increase in the negative moment and the shear at the adjacent interior bent. The existence of the settlements cannot be confirmed or rejected; however, inspection of the tabulated crack data does not indicate the the structures that have had these supposed settlements show a greater tendency toward cracking.

When considering either the shrinkage effects, which are significant, or the existence of settlements, again significant, one should keep in mind that either of these loadings probably accumulated on the structures

within the first five years after they were constructed (8). This means that these structures have carried traffic with these effects for at least fifteen years.

The horizontal cracks at the abutments at the approximate locations that the web attaches to the upper and lower flanges are not primarily caused by a stress condition. As noted previously, the two primary factors contributing to this cracking were the workmanship at the time these structures were built and the subsequent infiltration of drainage water from the structure along the construction joint. Freeze-thaw has helped to extend these cracks. The crack at the abutment at the mid-depth of the girder which passes horizontally through the diaphragm is considered to be a continuation of a diagonal shear crack and is helped to occur by the presence of shrinkage in the end diaphragm of the girder.

The abutment translations that have occurred are not contributing significantly to the cracking in the girder. The translation of the abutment is apparently the result of the way it was designed. In addition, the passive soil pressure is not adequate to stabilize the active soil pressure component. It is apparent that as frequently as these movements were observed, they cannot be explained by the occurrence of a local unusual situation.

It is not expected that the cracks or the conditions uncovered in this investiagtion will have a serious detrimental effect on the service life of these structures. A possible exception is if there is significant reinforcing steel corrosion in progress, particularly in the horizontal cracks that have occurred along the construction joint at the abutments. From the data taken it is not possible to tell how advanced the

corrosion is. The structure could tolerate a significant amount of corrosion in these areas before it would affect the integrity of the structure.

FUTURE STUDY

Field Observations

A systematic method of monitoring the cracks might be useful for verifying the causes which have been proposed in this paper and for continuously assessing the structural integrity of the bridges.

The field observations which were performed for this study were the first attempts at quantifying and categorizing the cracks, but the method of recording the observed cracks by sketching is subject to the interpretation of the observer. By selecting a small number of bridges for intensive, periodic observations, small changes in the cracks could be detected. The locations, widths, and lengths of cracks as they appear on the sides of the girder could be measured and recorded. Placing a mark at the end of a crack would verify either the growth or the stability of the crack upon later observation.

The possibility that the cracking resulted from support movements was not completely investigated by the writer because of the absence of related data. Precise measurements taken periodically which establish the vertical and horizontal position of each support could be used to determine whether or not the supports are moving. The degree to which the cracking is related to the support movements could then be tested by coupling the crack measurement data with the support movement data.

Analysis

The effects of concrete creep were not considered in the model, and these effects would have a significant effect on the structure (13).

Several methods of creep analysis have been derived which could be applied to this situation (14)(15).

Torsional loads were not considered in the model even though such loads could have contributed to the cracking. Torsional loads were probably not a primary cause of the observed cracks due to the torsional strength of the deep, multiple cell construction of the girder. However, the determination of the torsionally induced stresses in multiple cell reinforced concrete box girders is a problem worthy of study (16) (17).

A finite element (18) (19) study of the abutment-soil interaction would be useful for verifying the design of the abutment. A far more refined model than the frame analysis used in this study could be assembled using finite elements. Several finite element programs are available (18), including the finite element portion of the STRUDL program (20), which have the capabilities required by this problem.

LITERATURE CITED

1. Sowers, George B., and Sowers, George F, Introductory Soil Mechanics and Foundations, MacMillan Publishing Company, Inc., New York, N.Y., 3rd Edition, 1970.

2. Commentary on Building Code Requirements for Reinforced Concrete, American Concrete Institute, Report 318-77, Detroit, Michigan, 1977.

3. Logcher, Robert D., and Flachsbart, Barry B., and others, ICES STRUDL-II The Structural Design Language Engineering User's Manual, Volume 1, Frame Analysis, 1st Edition, Department of Civil Engineering, Massachusetts Institute of Technology, Cambridge, Massachusetts, November 1968.

4. Mcquire, W., and Gallagher, R.H., Matrix Structural Analysis, John Wiley and Sons, New York, N.Y., 1979.

5. McCormac, Jack C., Structural Analysis, Intext Education Publishers, New York, N.Y., 1975.

6. Standard Specifications for Highway Bridges, American Association of State Highway and Transportation Officials, Washington, D.C., 12th Edition, 1977.

7. Nelson, C.H., and Frie, O.C., "Lightweight Structural Concrete Proportioning and Control," American Concrete Institute Journal, 29, 605-21, January, 1958.

8. Guide for Structural Lightweight Aggregate Concrete, American Concrete Institute, Report 213R-9, Detroit, Michigan, 1979.

9. Design and Control of Concrete Mixtures, Portand Cement Association, USA, 12th Edition, 1979.

10. McNulty, James F., "Thrust Loading on Piles," Journal of the Soil Mechanics and Foundations Division, Proceedings of the American Society of Civil Engineers, 82, 940, April, 1952.

11. Moulton, L.K., and Kula, J.K., "Bridge Movements and Their Effects," Public Roads, United States Department of Transportation, Federal Highway Administration, 44, 62-75, September, 1980.

12. Winter, G., and Nilson, A.H., Design of Concrete Structures, McGraw-Hill Book Company, New York, N.Y., 8th Edition, 1972.

13. Scordelis, A.C., and others, "Time-Dependent Behavior of Concrete Box Girder Bridges," American Concrete Institute Journal, 76, 159-77, January, 1979.

14. Ganga Roa, Hota V.S., and Halvorsen, Grant T., Analytical Studies of the Effects of Movements on Steel and Concrete Bridges, "Public Roads, United States Department of Transportation, Federal Highway Administration, 44, 103-115, December, 1980.

15. Bronson, D.E., Deformation of Concrete Structures, McGraw-Hill Book Company, New York, N.Y., 1977.

16. Timoshenko, S., Theory of Elasticity, McGray-Hill Book Company, New York, N.Y., 1st Edition, 1934.

17. Rangan, B.V. Stanley, and Hall, "Behavior of Concrete Beams in Torsion and Bending" Journal of the Structural Division, Proceedings of the American Society of Civil Engineers, 103, 759-772, April, 1977.

18. Cook, Robert D., Concepts and Applications of Finite Element Analysis, John Wiley and Sons, New York, N.Y., 1974.

19. Zienkiewiez, O.C., The Finite Element Method, McGraw-Hill Book Company, New York, N.Y., 1979.

20. Logcher, Robert D., Connor, J., and Nelson, Mark F., and others, ICES STRUDL-II The Structural Design Language Engineering User's Manual, Volume 2, Additional Design and Analysis Facilities, 2nd Edition, Department of Civil Engineering, Massachusetts Institute of Technology, Cambridge, Massachusetts, June 1972.